

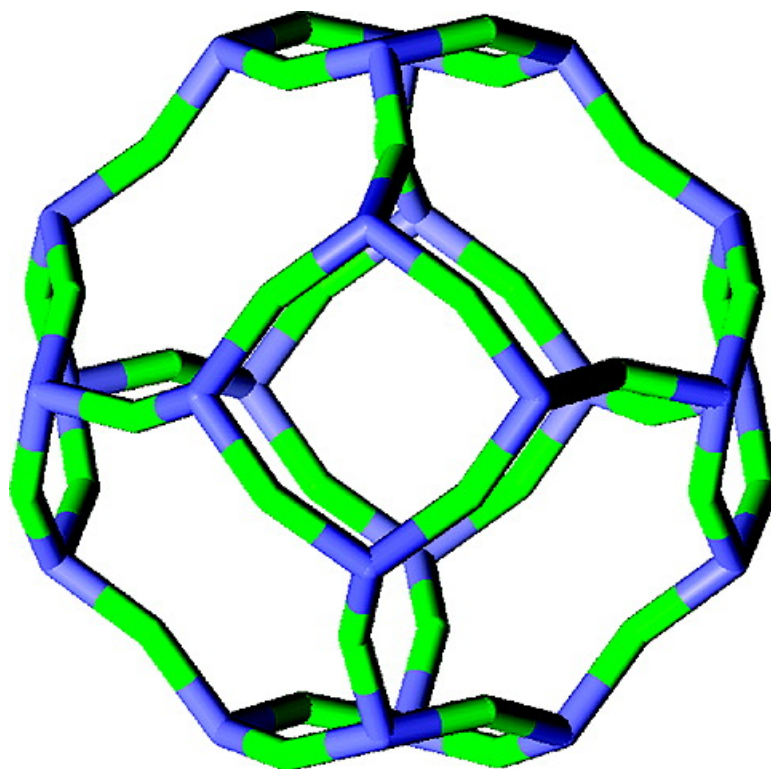
Article

## Isomorphism of Anhydrous Tetrahedral Halides and Silicon Chalcogenides: Energy Landscape of Crystalline BeF, BeCl, SiO, and SiS

Martijn A. Zwijnenburg, Furio Cora#, and Robert G. Bell

*J. Am. Chem. Soc.*, **2008**, 130 (33), 11082-11087 • DOI: 10.1021/ja8026967 • Publication Date (Web): 24 July 2008

Downloaded from <http://pubs.acs.org> on February 8, 2009



### More About This Article

Additional resources and features associated with this article are available within the HTML version:

- Supporting Information
- Links to the 1 articles that cite this article, as of the time of this article download
- Access to high resolution figures
- Links to articles and content related to this article
- Copyright permission to reproduce figures and/or text from this article



**ACS Publications**  
High quality. High impact.

[View the Full Text HTML](#)



# Isomorphism of Anhydrous Tetrahedral Halides and Silicon Chalcogenides: Energy Landscape of Crystalline $\text{BeF}_2$ , $\text{BeCl}_2$ , $\text{SiO}_2$ , and $\text{SiS}_2$

Martijn A. Zwijnenburg,<sup>\*,†,‡</sup> Furio Corà,<sup>§,||</sup> and Robert G. Bell<sup>§</sup>

*Departament de Química Física and Institut de Recerca de Química Teòrica i Computacional, Universitat de Barcelona, E-08028 Barcelona, Spain, Christopher Ingold Laboratories, Department of Chemistry, University College London, 20 Gordon Street, London WC1H 0AJ, United Kingdom, and Materials Simulation Laboratory, University College London, Gower Street, London, WC1E 6BT, United Kingdom*

Received April 12, 2008; E-mail: m.zwijnenburg@ub.edu

**Abstract:** We employ periodic density functional theory calculations to compare the structural chemistry of silicon chalcogenides (silica, silicon sulfide) and anhydrous tetrahedral halides (beryllium fluoride, beryllium chloride). Despite the different formal oxidation states of the elements involved, the divalent halides are known experimentally to form crystal structures similar to known  $\text{SiX}_2$  frameworks; the rich polymorphic chemistry of  $\text{SiO}_2$  is however not matched by divalent halides, for which a very limited number of polymorphs are currently known. The calculated energy landscapes yield a quantitative match between the relative polymorphic stability in the  $\text{SiO}_2/\text{BeF}_2$  pair, and a semiquantitative match for the  $\text{SiS}_2/\text{BeCl}_2$  pair. The experimentally observed polymorphs are found to lie lowest in energy for each composition studied. For the two  $\text{BeX}_2$  compounds studied, polymorphs not yet synthesized are predicted to lie very low in energy, either slightly above or even in between the energy of the experimentally observed polymorphs. The experimental lack of polymorphism for tetrahedral halide materials thus does not appear to stem from a lack of low-energy polymorphs but more likely is the result of a lack of experimental exploration. Our calculations further indicate that the rich polymorphic chemistry of  $\text{SiO}_2$  can be potentially matched, if not extended, by  $\text{BeF}_2$ , provided that milder synthetic conditions similar to those employed in zeolite synthesis are developed for  $\text{BeF}_2$ . Finally, our work demonstrates that both classes of materials show the same behavior upon replacement of the 2p anion with the heavier 3p anion from the same group; the thermodynamic preference shifts from structures with large rings to structures with larger fractions of small two and three membered rings.

## I. Introduction

Tetrahedral framework materials, in which 4-coordinated cations (T) are linked by 2-coordinated anions (X) to yield an extended network of composition  $\text{TX}_2$ , are known in the form of oxides ( $\text{SiO}_2$ ,  $\text{GeO}_2$ , potentially  $\text{CO}_2$  under applied pressure), sulfides ( $\text{SiS}_2$ ,  $\text{GeS}_2$ ), and selenides ( $\text{SiSe}_2$ ,  $\text{GeSe}_2$ ). However, besides these well-known examples where T is a tetravalent element from the carbon group and X a divalent chalcogenide ( $\text{T}^{4+}\text{X}^{2-}$ ), a whole range of crystalline  $\text{TX}_2$  materials are known where X is a halide and T a divalent cation from either the alkali earths<sup>1,2</sup> ( $\text{BeF}_2$ ,  $\text{BeCl}_2$ ,  $\text{BeBr}_2$ ,  $\text{BeI}_2$ ) or from the zinc group<sup>3-8</sup> ( $\text{ZnCl}_2$ ,  $\text{ZnBr}_2$ ,  $\text{ZnI}_2$ ,  $\text{HgBr}_2$ ,  $\text{HgI}_2$ ). Despite the different

formal oxidation states of the elements involved, these  $\text{T}^{2+}\text{X}^{2-}$  materials typically crystallize in polymorphs that have a similar topology as known  $\text{T}^{4+}\text{X}^{2-}$  materials (by topology we refer here to the way in which the corner-sharing  $\text{TX}_4$  tetrahedra connect to each other to form a three or lower-dimensional framework). For example, anhydrous  $\text{BeF}_2$  is known to crystallize in the quartz topology<sup>1</sup> (isomorphic to  $\text{SiO}_2$  and  $\text{GeO}_2$  quartz, see Figure 1), and one of the two polymorphs synthesized for anhydrous  $\text{BeCl}_2$ ,  $\text{BeBr}_2$ , and  $\text{BeI}_2$  (the  $\alpha$ -phase,<sup>2</sup> see Figure 2) has the same topology as orthorhombic  $\text{SiS}_2/\text{SiSe}_2$ <sup>9</sup> and a rare form of silica (silica- $\text{W}^{10}$ ). These structural similarities between  $\text{T}^{4+}\text{X}^{2-}$  and  $\text{T}^{2+}\text{X}^{2-}$  materials extend beyond the crystalline polymorphs:  $\text{BeF}_2$ <sup>11,12</sup> and  $\text{BeCl}_2$ ,<sup>13</sup> for example, are

<sup>†</sup> Universitat de Barcelona.

<sup>‡</sup> Formerly at: Davy Faraday Research Laboratory, third Floor, Kathleen Lonsdale Building, University College London, Gower Street, London, WC1E 6BT, United Kingdom.

<sup>§</sup> Department of Chemistry, University College London.

<sup>||</sup> Materials Simulation Laboratory, University College London.

- (1) Wright, A. F.; Fitch, A. N.; Wright, A. C. *J. Solid State Chem.* **1988**, *73*, 298.
- (2) Troyanov, S. I.; Russ, J. *Inorg. Chem.* **2000**, *45*, 1481.
- (3) Brynestad, J.; Yake, H. L. *Inorg. Chem.* **1978**, *17*, 1376.
- (4) Fourcroy, P. H.; Carre, D.; Rivet, J. *Acta Crystallogr.* **1978**, *B34*, 3160.
- (5) Chieh, C.; White, M. A. *Z. Kristallogr.* **1984**, *166*, 189.

- (6) Hostettler, M.; Schwarzenbach, D. *C. R. Chem.* **2005**, *8*, 147.
- (7) Hostettler, M.; Birkedal, H.; Schwarzenbach, D. *Acta Crystallogr. B* **2002**, *58*, 903.
- (8) Hostettler, M.; Schwarzenbach, D. *Acta Crystallogr. B* **2002**, *58*, 914.
- (9) Peters, J.; Krebs, B. *Acta Crystallogr. B* **1982**, *38*, 1270.
- (10) Weiss, A.; Weiss, A. *Z. Anorg. Allg. Chem.* **1954**, *276*, 95.
- (11) Galeener, F. L.; Leadbetter, A. J.; Stringfellow, M. W. *Phys. Rev. B* **1983**, *27*, 1052.
- (12) Wright, A. C.; Clare, A. G.; Etherington, G.; Sinclair, R. N.; Brawer, S. A.; Weber, M. J. *J. Non-Cryst. Solids* **1989**, *111*, 139.
- (13) Pavlou, E. A.; Papatheodorou, G. N. *Phys. Chem. Chem. Phys.* **2000**, *2*, 1035.

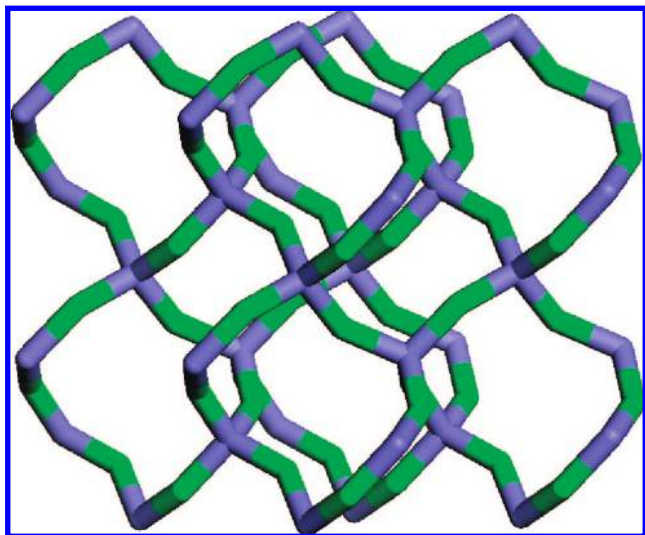


**Figure 1.** Fragment of the BeF<sub>2</sub> quartz structure (beryllium atoms in blue and fluorine atoms in green).

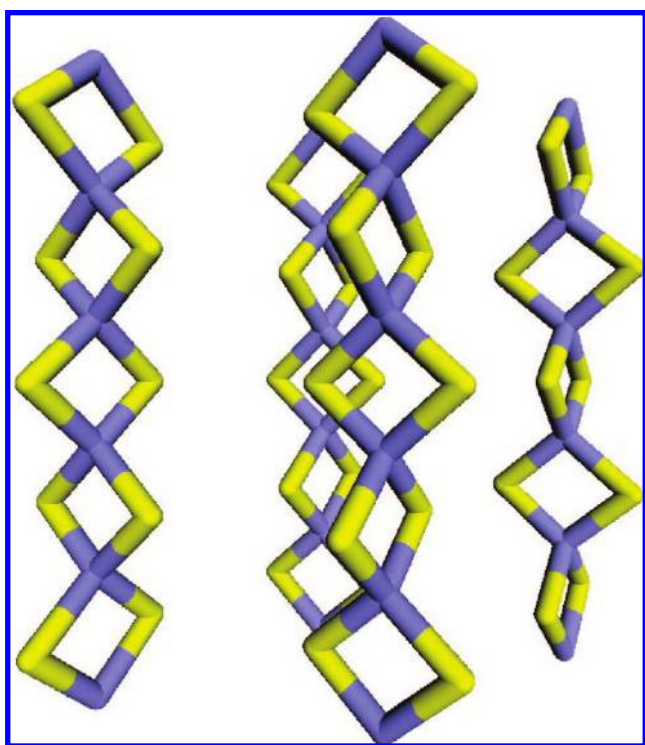


**Figure 2.** Fragment of the  $\alpha$ -BeCl<sub>2</sub> structure clearly showing the constituting chains (beryllium atoms in blue and chlorine atoms in yellow).

known to form amorphous phases with an average structure as probed by neutron diffraction and/or Raman spectroscopy that is similar to that of vitreous SiO<sub>2</sub> and SiS<sub>2</sub>, respectively.

For each of the T<sup>2+</sup>X<sup>2-</sup> materials, typically only one or two crystalline polymorphs have been prepared experimentally (please note that for some systems more polymorphs were reported in the past; however, often the crystal structure of these polymorphs were not refined and/or their synthesis was never repeated, and as a result, their identification is rather tentative, e.g., the BeF<sub>2</sub> analogs of the coesite<sup>14</sup> and cristobalite<sup>15</sup>

minerals), in contrast with silica for which experimentally more than 40 different polymorphs are known.<sup>16</sup> This might, however, be similar to the situation for SiS<sub>2</sub>, for which also only two polymorphs have been synthesized but for which recent theoretical work suggests there are many more potential polymorphs awaiting discovery.<sup>17</sup> The above comparison raises the question as to whether the observed absence of polymorphism in anhydrous tetrahedral halides has a physical origin, e.g. a large energetic difference between the different framework structures, or stems from a lack of experimental exploration.

The relative energies of different T<sup>2+</sup>X<sup>2-</sup> framework structures can be reliably determined computationally, making reference to known T<sup>4+</sup>X<sup>2-</sup> networks to identify alternative T<sup>2+</sup>X<sup>2-</sup> structures. To understand the observed similarities and differences in polymorphism between T<sup>2+</sup>X<sup>2-</sup> and T<sup>4+</sup>X<sup>2-</sup> materials, and to rationalize why a particular polymorph is found for a particular chemical composition, one needs to consider the relative (free) energies of the different possible polymorphs for each composition. In the absence of strong kinetic effects one would expect to form the polymorph that lies lowest in (free) energy. Moreover, for crystalline solids, the entropic contribution is often small (as explicitly demonstrated for silica<sup>18</sup>) so that the free energy is well approximated by the enthalpy. In contrast to the ample thermodynamic data available for silica, obtained from both experiment<sup>19</sup> and theory,<sup>20–25</sup> the energetic ordering of different T<sup>2+</sup>X<sup>2-</sup> polymorphs is generally unknown. The exception being the nonhalide BeH<sub>2</sub> for which the relative (free) energies of several polymorphs have been studied computationally<sup>26–28</sup> by different groups due to the potential application of alkali hydrides in hydrogen storage; more limited theoretical work is also available on the  $\alpha \rightarrow \beta$  transition in BeF<sub>2</sub> quartz<sup>29</sup> and on the BeCl<sub>2</sub> melt.<sup>30</sup>

Following our earlier work on SiS<sub>2</sub>,<sup>17</sup> we here employ periodic density functional theory (DFT) calculations to evaluate the relative energies of a whole series of possible polymorphs for two characteristic T<sup>2+</sup>X<sup>2-</sup> materials: anhydrous BeF<sub>2</sub> and BeCl<sub>2</sub>. The polymorphs studied include the experimentally observed polymorphs for BeF<sub>2</sub> and BeCl<sub>2</sub> (besides the  $\alpha$ -phase discussed above, we also consider the  $\beta$ -phase,<sup>2</sup> which corresponds to two interpenetrating supertetrahedral versions of the

- (16) Wragg, D. S.; Morris, R. E.; Burton, A. W. *Chem. Mater.* **2008**, *20*, 1561.
- (17) Zwijnenburg, M. A.; Corà, F.; Bell, R. G. *J. Am. Chem. Soc.* **2007**, *129*, 12588.
- (18) Piccione, P. M.; Woodfield, B. F.; Boerio-Goates, J.; Navrotsky, A.; Davis, M. E. *J. Phys. Chem. B* **2001**, *105*, 6025.
- (19) Piccione, P. M.; Laberty, C.; Yang, S. Y.; Cambor, M. A.; Navrotsky, A.; Davis, M. E. *J. Phys. Chem. B* **2000**, *104*, 10001.
- (20) Henson, N. J.; Cheetham, A. K.; Gale, J. D. *Chem. Mater.* **1994**, *6*, 1647.
- (21) Civalleri, B.; Zicovich-Wilson, C. M.; Ugliengo, P.; Saunders, V. R.; Dovesi, R. *Chem. Phys. Lett.* **1998**, *292*, 394.
- (22) Catti, M.; Civalleri, B.; Ugliengo, P. *J. Phys. Chem. B* **2000**, *104*, 7259.
- (23) Astala, R.; Auerbach, S. M.; Monson, P. A. *J. Phys. Chem. B* **2004**, *108*, 9208.
- (24) Zwijnenburg, M. A.; Corà, F.; Bell, R. G. *J. Phys. Chem. B* **2007**, *111*, 6156.
- (25) Bromley, S. T.; Moreira, I.D.P.R.; Illas, F.; Wojdel, J. C. *Phys. Rev. B* **2006**, *73*, 134202.
- (26) Hantsch, U.; Winkler, B.; Milman, V. *Chem. Phys. Lett.* **2003**, *378*, 343.
- (27) Vajeeston, P.; Ravindran, P.; Kjekshus, A.; Fjellvag, H. *Appl. Phys. Lett.* **2004**, *84*, 34.
- (28) Hector, L. G.; Herbst, J. F.; Wolf, W.; Saxe, P.; Kresse, G. *Phys. Rev. B* **2007**, *76*, 014121.
- (29) Takada, A.; Richet, P.; Catlow, C. R. A.; Price, G. D. *J. Non-Cryst. Solid* **2007**, *353*, 1892.
- (30) Wilson, M.; Madden, P. A. *Mol. Phys.* **1997**, *92*, 197.

(14) Dachille, F.; Roy, R. Z. *Krist.* **1959**, *111*, 451.

(15) Brandenberger, E. *Schweiz. Min. Petrog. Mitt.* **1932**, *12*, 243.



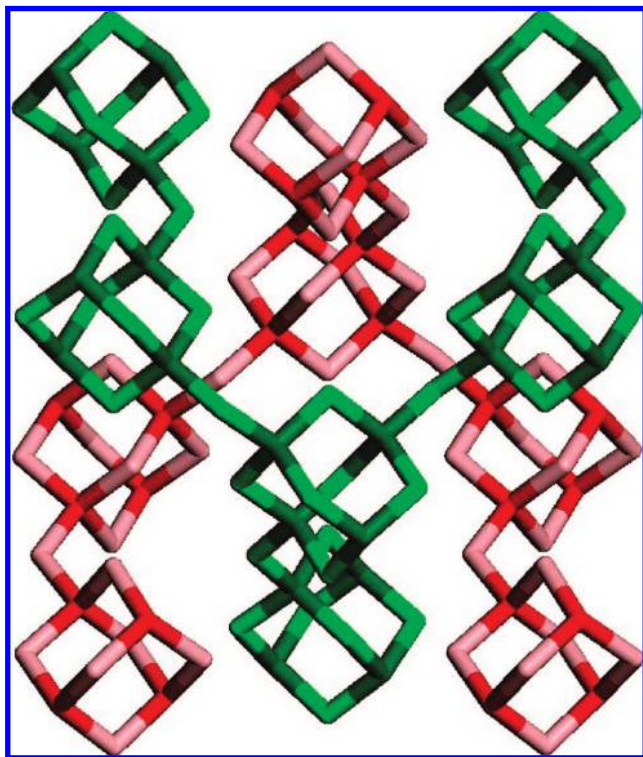


**Figure 3.** Fragment of the  $\beta$ -BeCl<sub>2</sub> crystal structure clearly showing the two interpenetrating supertetrahedral cristobalite frameworks.

diamond framework, see Figure 3) and six model crystalline materials whose topologies correspond to the dense frameworks cristobalite (diamond topology) and coesite, and the nanoporous frameworks SOD, CHA, OSO, and RWY. For comparison, we also performed similar calculations on SiO<sub>2</sub> and SiS<sub>2</sub> versions of the same topologies (values where possible taken from ref 17). The structures were optimized using a hybrid-exchange density functional that included a fixed amount of Hartree–Fock exchange. For all structures the gamma point phonons are calculated. The latter not only allow us to extract additional data, but also to verify that all optimized structures are true minima with respect to the internal coordinates. This feature is important as the absence of an experimental structure for some materials means that their starting structure could only be approximated and thus may optimize to n-order saddle points if left unchecked.

## II. Computational Methodology

The materials discussed in the paper have been investigated with periodic DFT calculations, employing the hybrid PBE0<sup>31</sup> density functional and localized orbitals, as implemented in the CRYSTAL06<sup>32</sup> code. The basis sets employed are expressed in a series of Gaussian type functions and are generally of double valence

plus polarization quality for each atomic species (Be,<sup>33</sup> F,<sup>34</sup> Cl,<sup>35</sup> Si and O,<sup>36</sup> and S<sup>37</sup>). All elements are treated at the all-electron level.

We used a Monkhorst-Pack grid of  $8 \times 8 \times 8$  and truncation thresholds of (7 7 7 14) for the Coulomb and exchange series,<sup>32</sup> while SCF convergence thresholds were set to  $1 \times 10^{-8}$  hartree for both eigenvalues and total energies. These tolerances ensure high numerical accuracy in the calculations. Geometry optimizations were restarted until the lattice parameters showed no further change and were checked against the root-mean-square (rms) and absolute value of the largest component for both gradients and nuclear displacements. Optimization was considered complete when the four conditions were simultaneously satisfied for both fractional coordinates and unit cell parameters, using the tight values of  $1.2 \times 10^{-5}$  for the maximum gradient and  $1.8 \times 10^{-5}$  for the maximum displacement (all in a.u.).

Gamma point phonons of the optimized structures were calculated using numerical differentiation of the analytical gradients of the energy with respect to the atomic displacements,<sup>38,39</sup> where the second derivatives are calculated using a three-point formula and Cartesian displacements of 0.01 Å. Following Pascale<sup>38</sup> and Zicovich-Wilson<sup>39</sup> (who investigated the effect of computational parameters such as basis-set and integration grid on the calculated spectra), we tested our approach by comparing the calculated and experimental phonon spectra at the gamma point of  $\alpha$ -quartz, for which high quality experimental data<sup>40</sup> is available, and found (see Supporting Information) that the match between theory and experiment is good with a rms difference of  $11 \text{ cm}^{-1}$ .

Finally, Born effective charge tensors<sup>41</sup> for the different materials were obtained through the use of localized Wannier functions.<sup>42,43</sup> This tensor is the first derivative of the polarization per unit-cell with respect to atomic displacements at zero external electric field and is linked to the intensity of infrared modes. As such, it and the associated Born effective charges (defined as 1/3 of the trace of the Born effective charge tensors) are experimental observables (this in contrast to more routinely used theoretically obtained charges e.g. Mulliken) and reflect the coupling between phonons and the long-range Madelung field in a solid.

## III. Results and Discussion

As a first test of the applied methodology, we compare the DFT predicted and experimental geometries for quartz-structured BeF<sub>2</sub> and  $\alpha$ -BeCl<sub>2</sub>. The data in Table 1 show that overall the geometry differences are small (below 1.5%) with exception of the *a* and *b* lattice parameters of  $\alpha$ -BeCl<sub>2</sub>, which are considerably overestimated. The latter is a direct result of the fact that  $\alpha$ -BeCl<sub>2</sub> has a one-dimensional chain structure, and the *a* and *b* lattice parameters refer to interchain interactions which are dominated by dispersion forces not properly represented in DFT. The same effect is present in orthorhombic SiS<sub>2</sub>, where however we found that distortions along the *a* and *b* directions are very soft degrees of freedom, and the calculated

- (31) Adamo, C.; Barone, V. *J. Chem. Phys.* **1999**, *110*, 6158.  
 (32) Dovesi, R.; Saunders, V. R.; Roetti, C.; Orlando, R.; Zicovich-Wilson, C. M.; Pascale, F.; Civalleri, B.; Doll, K.; Harrison, N. M.; Bush, I. J.; D'Arco, Ph.; Llunell, M. *CRYSTAL06 User's Manual*; Università di Torino: Torino, 2006.  
 (33) Lichanot, A.; Chaillet, M.; Larrieu, C.; Dovesi, R.; Pisani, C. *Chem. Phys.* **1992**, *164*, 383.  
 (34) Valerio, G.; Catti, M.; Dovesi, R.; Orlando, R. *Phys. Rev. B* **1995**, *52*, 2422.

- (35) Harrison, N. M.; Saunders, V. R. *J. Phys. Condens. Matter* **1992**, *4*, 3873.  
 (36) Zicovich-Wilson, C. M.; Dovesi, R. *J. Mol. Catal. A: Chem.* **1997**, *119*, 449.  
 (37) Catti, M. *Phys. Rev. B* **2002**, *65*, 224115.  
 (38) Pascale, F.; Zicovich-Wilson, C. M.; Lopez Gejo, F.; Civalleri, B.; Orlando, R.; Dovesi, R. *J. Comput. Chem.* **2004**, *25*, 888.  
 (39) Zicovich-Wilson, C. M.; Pascale, F.; Roetti, C.; Saunders, V. R.; Orlando, R.; Dovesi, R. *J. Comput. Chem.* **2004**, *25*, 1873.  
 (40) Scott, J. F.; Porto, S. P. S. *Phys. Rev.* **1967**, *161*, 903.  
 (41) Born, M.; Huang, K. *Dynamical theory of crystal lattices*; Clarendon: Oxford, 1954.  
 (42) Zicovich-Wilson, C. M.; Dovesi, R.; Saunders, V. R. *J. Chem. Phys.* **2001**, *115*, 9708.  
 (43) Zicovich-Wilson, C. M.; Bert, A.; Roetti, C.; Dovesi, R.; Saunders, V. R. *J. Chem. Phys.* **2002**, *116*, 1120.

**Table 1.** PBE0 Optimized Structural Parameters for BeF<sub>2</sub> Quartz and  $\alpha$ -BeCl<sub>2</sub> Polymorphs<sup>a</sup>

	BeF <sub>2</sub> quartz	BeF <sub>2</sub> coesite	$\alpha$ -BeCl <sub>2</sub>	$\alpha$ -BeCl <sub>2</sub> isolated chain
<i>a</i>	4.786 (4.7239)	6.971 (6.88)	5.600 (5.285)	
<i>b</i>		12.026 (11.92)	10.810 (9.807)	
<i>c</i>	5.244 (5.1788)	6.962 (6.88)	5.257 (5.227)	5.250
$\beta$		120.02 (120)		
$\langle \text{Be-X} \rangle$	1.556 (1.543)		2.031 (2.026)	2.031
$\langle \text{Be-X-Be} \rangle$	145.7 (144.6)		80.6 (80.3)	80.5

<sup>a</sup> Experimental parameters from refs 1, 2, 14 in brackets.

**Table 2.** PBE0 Calculated Relative Energies for SiO<sub>2</sub>, BeF<sub>2</sub>, SiS<sub>2</sub>, and BeCl<sub>2</sub> Materials<sup>a</sup>

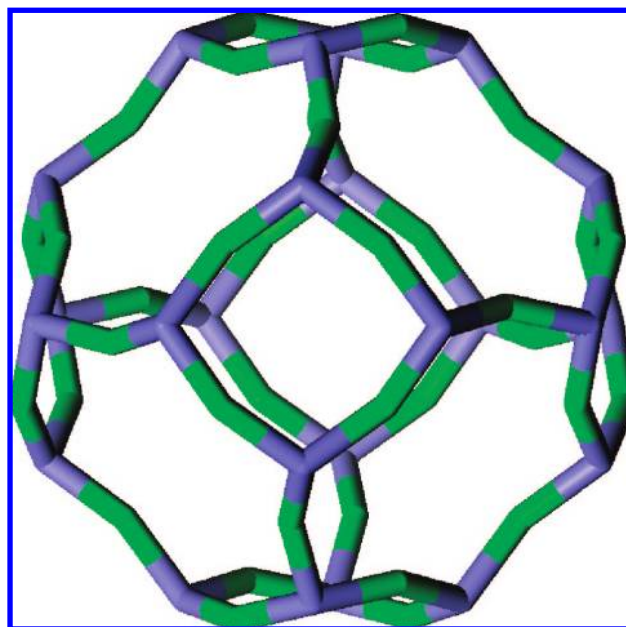
	SiO <sub>2</sub>	BeF <sub>2</sub>	SiS <sub>2</sub>	BeCl <sub>2</sub>
qtz	<b>0</b>	<b>0</b>	0	0
día	<b>2</b>	1	-33	-13
coe	<b>4</b>	<b>2</b>	34	12
SOD	<b>7</b>	5	-31	-12
CHA	<b>9</b>	5	0	1
OSO	21	11	-34	-13
$\beta$ -BeCl <sub>2</sub>	43	18	-37	-17
RWY	46	21	-37	-16
$\alpha$ -BeCl <sub>2</sub>	119	58	-47	-16

<sup>a</sup> Energy of quartz polymorph arbitrarily set to zero for all materials, experimentally known polymorphs in bold, and all energies in kJ/mol TX<sub>2</sub>.

error in the *a* and *b* lattice parameters does not affect the relative stability of polymorphs. The *c* lattice parameter of  $\alpha$ -BeCl<sub>2</sub>, which lies along the chain direction, and the intrachain geometric parameters are instead very well reproduced by DFT, and the geometry of an isolated chain (*a* and *b* set to 100 Å) is virtually identical to that of a chain in the crystal. Finally, for BeF<sub>2</sub> Coesite,<sup>14</sup> whose synthesis was reported but for which the crystal structure was never refined, we find an excellent match with the published experimental cell parameters (differences again below 1.5%), strongly supporting the experimental identification.

Building on the above result, we optimized the structures of nine different BeF<sub>2</sub> and BeCl<sub>2</sub> frameworks. For each material studied, the calculated phonon spectrum at the gamma point shows no imaginary modes after optimization. Each structure considered here is therefore a proper minimum in the potential energy surface, at least with respect to symmetry-lowering phase transitions that can be described within the unit cell employed in the calculations. The calculated relative energies of the different structures are presented in Table 2, where we observe a number of features.

First it is important to note that for all materials the experimentally known polymorphs are correctly recovered as the lowest energy structures. Moreover, in the case of BeCl<sub>2</sub>, for which two polymorphs are known experimentally, both polymorphs are found to lie very close in energy. Just as for SiS<sub>2</sub> there is no theoretical evidence for a sparse polymorph energy spectrum. In contrast, if one takes into account that the nine frameworks studied are merely the top of the proverbial iceberg, with currently more than 100,000 hypothetical TX<sub>2</sub> frameworks having been enumerated computationally,<sup>44–53</sup> the

**Figure 4.** Fragment of the BeF<sub>2</sub> sodalite structure clearly showing the porous cages present (beryllium atoms in blue and fluorine atoms in green).

polymorph energy spectrum of BeX<sub>2</sub>, and of tetrahedral anhydrous halides in general, is thus very likely to comprise several structures in an accessible energy range. The lack of experimental observation of polymorphism in anhydrous halides appears thus not to be thermodynamic in origin, but most likely is the result of the relatively undirected methods employed in the synthesis of anhydrous halides (crystallization from melt or chemical vapor transport) compared with those used for silicates, where organic template molecules are often used to direct the synthesis toward a particular metastable polymorph.

A second observation is that for both BeX<sub>2</sub> compounds studied, polymorphs not yet synthesized are found to lie very low in energy, either slightly above (e.g., BeF<sub>2</sub> cristobalite and sodalite and BeCl<sub>2</sub> OSO) or even in between (BeCl<sub>2</sub> RWY) the energies of experimentally observed polymorphs. This suggests that if for example a low temperature route toward the synthesis of anhydrous halides is developed, that enables the use of organic template molecules (which are not stable at the high temperatures required for crystallization from melt or chemical vapor transport) porous polymorphs of anhydrous halides (see Figure 4) are within the realm of possibilities.

A third observation is that a very close match exists between the calculated order of stability of BeF<sub>2</sub> polymorphs with that of the corresponding SiO<sub>2</sub> structures, and of BeCl<sub>2</sub> with SiS<sub>2</sub>. The experimentally observed similarities in polymorphism between T<sup>2+</sup>X<sub>2</sub><sup>-</sup> and T<sup>4+</sup>X<sub>2</sub><sup>2-</sup> materials highlighted in the

(44) Treacy, M. M. J.; Randall, K. H.; Rao, S.; Perry, J. A.; Chadi, D. J. *Z. Kristallogr.* **1997**, *212*, 768.

(45) Delgado Friedrichs, O.; Dress, A. W. M.; Huson, D. H.; Klinowski, J.; Mackay, A. L. *Nature* **1999**, *400*, 644.

(46) Mellot-Draznics, C.; Girard, S.; Ferey, G. *J. Am. Chem. Soc.* **2002**, *124*, 15326.

(47) Foster, M. D.; Simperler, A.; Bell, R. G.; Delgado Friedrichs, O.; Almeida Paz, F. A.; Klinowski, J. *Nat. Mater.* **2004**, *3*, 234.

(48) Treacy, M. M. J.; Rivin, I.; Balkovsky, E.; Randall, K. H.; Foster, M. D. *Microporous Mesoporous Mater.* **2004**, *74*, 121.

(49) Foster, M. D.; Delgado Friedrichs, O.; Bell, R. G.; Almeida Paz, F. A.; Klinowski, J. *J. Am. Chem. Soc.* **2004**, *126*, 9769.

(50) Woodley, S. M.; Catlow, C. R. A.; Battle, P. D.; Gale, J. D. *Chem. Commun.* **2004**, 22.

(51) Simperler, A.; Foster, M. D.; Delgado Friedrichs, O.; Bell, R. G.; Almeida Paz, F. A.; Klinowski, J. *Acta Crystallogr. B* **2005**, *61*, 263.

(52) Earl, D. J.; Deem, M. W. *Ind. Eng. Chem. Res.* **2006**, *45*, 5449.

(53) Wojdel, J. C.; Zwijnenburg, M. A.; Bromley, S. T. *Chem. Mater.* **2006**, *18*, 1464.

**Table 3.** T–X–T Angles for the PBE0 Optimized Geometries of the SiO<sub>2</sub>, BeF<sub>2</sub>, SiS<sub>2</sub>, and BeCl<sub>2</sub> Materials

	SiO <sub>2</sub>	BeF <sub>2</sub>	SiS <sub>2</sub>	BeCl <sub>2</sub>
qtz	141	146	119	127
dia	141	143	112	118
coe	147	150	128	136
SOD	144	152	111	117
CHA	147	150	117	124
OSO	129	130	107	113
RWY	123	127	105	110
α-BeCl <sub>2</sub>	91	89	81	81

introduction are mirrored therefore in the energy landscape of a wider range of structures.

Let us consider first the analogy between BeF<sub>2</sub> and SiO<sub>2</sub>: both crystallize in the quartz structure and for both materials this is found to be the lowest energy polymorph. Moreover, both materials are found to have the same energetic ordering of the polymorphs studied, where frameworks with large numbers of six-membered rings (rings involving six tetrahedral atoms) lie low in energy and frameworks with increasing fractions of three-membered and two-membered rings lie high in energy. The energetic match is quantitative: a good linear correlation ( $R^2 = 0.998$ ) is observed between the relative energies of the two materials, and perhaps the most important feature is that the energetic instability of a given BeF<sub>2</sub> polymorph with respect to quartz is only approximately half-that of the corresponding SiO<sub>2</sub> framework.

Similar trends emerge when comparing BeCl<sub>2</sub> and SiS<sub>2</sub>: both crystallize in the chain structure, and for both materials this is one of the three structures with lowest calculated energies, together with the β-BeCl<sub>2</sub> structure which has been observed experimentally for BeCl<sub>2</sub> but not yet for SiS<sub>2</sub>, and the RWY structure synthesized as a gallium germanium sulfide material. These three polymorphs all have small rings in the structure, and lie within 2 kJ/mol for BeCl<sub>2</sub>. BeCl<sub>2</sub> and SiS<sub>2</sub> materials have a similar energetic ordering among the nine polymorphs examined here, and again the energy penalty for unstable structures in BeCl<sub>2</sub> is approximately half that calculated for SiS<sub>2</sub>; as in the case for SiO<sub>2</sub>/BeF<sub>2</sub>, a good linear correlation between the calculated energies of the two materials is observed ( $R^2 = 0.979$ ).

Analogies can be found not only comparing a T<sup>2+</sup>X<sup>2-</sup> material with the corresponding T<sup>4+</sup>X<sup>2-</sup> compound in which the anion belongs to the same period of the periodic table, but also comparing the behavior of T<sup>2+</sup>X<sup>2-</sup> and T<sup>4+</sup>X<sup>2-</sup> materials upon substitution of the anions X with heavier elements from the same group (i.e., O → S and F → Cl). Frameworks with small rings are stabilized by the 3p anions, at the expense of frameworks with only larger rings that are preferentially observed for the 2p anions.

The similarities between T<sup>2+</sup>X<sup>2-</sup> and T<sup>4+</sup>X<sup>2-</sup> materials are not limited to the energy landscape. A comparison of the predicted geometries for the different materials, summarized in Tables 3 and 4, shows that parallel to the similarities in polymorphism and energetics, the T–X–T angles and T–X bond lengths of SiO<sub>2</sub> and BeF<sub>2</sub> are very alike, as are those of SiS<sub>2</sub> and BeCl<sub>2</sub>. In line with a previous study that was limited to quartz-like structures,<sup>54</sup> for all polymorphs studied, the T–X–T angles decrease in the order of BeF<sub>2</sub> ≥ SiO<sub>2</sub> ≫ BeCl<sub>2</sub> ≥ SiS<sub>2</sub>, with the SiO<sub>2</sub>/BeF<sub>2</sub> values consistently lying above the SiS<sub>2</sub>/

**Table 4.** T–X Bond Lengths (in Angstrom) for Selected PBE0 Optimized Polymorphs of the SiO<sub>2</sub>, BeF<sub>2</sub>, SiS<sub>2</sub>, and BeCl<sub>2</sub> Materials

	SiO <sub>2</sub>	BeF <sub>2</sub>	SiS <sub>2</sub>	BeCl <sub>2</sub>
qtz	1.63	1.56	2.16	2.05
SOD	1.62	1.55	2.15	2.04
α-BeCl <sub>2</sub>	1.67	1.58	2.15	2.03

**Table 5.** Polarization Fractions and Born Effective Charges of SiO<sub>2</sub>, BeF<sub>2</sub>, SiS<sub>2</sub>, and BeCl<sub>2</sub> Quartz

	P	Z*	
		T	X
SiO <sub>2</sub>	0.51	3.41	−1.70
BeF <sub>2</sub>	0.61	1.85	−0.92
SiS <sub>2</sub>	0.23	3.14	−1.56
BeCl <sub>2</sub>	0.44	1.94	−0.97

BeCl<sub>2</sub> values (by as much as 30°), while the bond lengths increase in the order BeF<sub>2</sub> < SiO<sub>2</sub> ≪ BeCl<sub>2</sub> < SiS<sub>2</sub>. As for the energy landscapes, the structural features of T<sup>2+</sup>X<sup>2-</sup> and T<sup>4+</sup>X<sup>2-</sup> materials therefore show the same trend upon substitution of the anion X with heavier elements of the same group.

The analogy highlighted above in the energetic and structural features of T<sup>2+</sup>X<sup>2-</sup> and T<sup>4+</sup>X<sup>2-</sup> materials holds also for the chemical bonding. A Boys localization of the valence Bloch orbitals to yield maximally localized Wannier functions shows that in all materials the T atoms are bonded by four (virtually) indistinguishable single σ-like orbitals with the four neighboring X anions. The Wannier functions corresponding to the T–X valence molecular orbitals are centered along the T–X direction and have contributions from both the T and X atoms, while their centers of charge are shifted away from the middle of the bond toward the more electronegative X atom. The magnitude of this shift, as defined by the polarization fraction P reported in Table 5 ( $P = 0$  is the covalent limiting case with the center of charge lying exactly in the middle of the bond, and  $P = 1$  is the ionic limiting case with the charge centered on the most electronegative atom in the bond), suggests that both T<sup>2+</sup>X<sup>2-</sup> and T<sup>4+</sup>X<sup>2-</sup> materials are semi-ionic in nature and that the bonding becomes more “covalent” with heavier anions. The Born effective charges parallel the formal oxidation states of the elements involved, and are roughly twice as large in T<sup>4+</sup>X<sup>2-</sup> than in T<sup>2+</sup>X<sup>2-</sup> materials. We believe that the different effective charges in T<sup>4+</sup>X<sup>2-</sup> and in T<sup>2+</sup>X<sup>2-</sup> frameworks are the main origin of the smaller energy differences between polymorphs observed for T<sup>2+</sup>X<sup>2-</sup> materials compared to T<sup>4+</sup>X<sup>2-</sup> materials. The roughly double effective charges in the latter increase the long-range Madelung potential in the lattice, and the associated electrostatic contribution to the total energy which shifts the low density T<sup>4+</sup>X<sup>2-</sup> materials up in energy relative to their T<sup>2+</sup>X<sup>2-</sup> counterparts.

Finally, two of the lowest energy frameworks of BeCl<sub>2</sub> display interesting variants on the (quasi) rigid unit modes that are commonly observed in silicates.<sup>55–57</sup> These are low energy phonon modes ( $0 < \omega < 1$  THz), in which the TX<sub>4</sub> tetrahedra move as almost rigid units. β-BeCl<sub>2</sub> shows an isolated quasi rigid unit mode at 29 cm<sup>−1</sup> (0.87 THz), which corresponds to

(55) Swainson, I. P.; Dove, M. T. *Phys. Rev. Lett.* **1993**, *71*, 193.(56) Hammonds, K. D.; Dove, M. T.; Giddy, A. P.; Heine, V.; Winkler, B. *Am. Mineral.* **1996**, *81*, 1057.(57) Hammond, K. D.; Deng, H.; Heine, V.; Dove, M. T. *Phys. Rev. Lett.* **1997**, *78*, 3701.(54) Zwijnenburg, M. A.; Huenerbein, R.; Bell, R. G.; Corà, F. *J. Solid State Chem.* **2006**, *179*, 3429.



a rigid translation of the two interpenetrating frameworks relative to each other along the *c* lattice vector. This mode is an antiphase combination of the acoustic modes of the isolated subframeworks along the *c* direction. The BeCl<sub>2</sub> version of the RWY framework shows instead two pairs of triply degenerate rigid unit modes at 26 and 27 cm<sup>-1</sup> (0.79 and 0.82 THz) in which not only the BeCl<sub>4</sub> tetrahedra but also the Be<sub>4</sub>Cl<sub>6</sub> supertetrahedra formed from them appear to remain rigid in the lattice vibration.

In summary, we have highlighted similarities at three levels between tetrahedral T<sup>2+</sup>X<sup>2-</sup> and T<sup>4+</sup>X<sup>2-</sup> materials, concerning the energy landscape of the respective polymorphs, and their structural and bonding features. A close match of properties exists between tetrahedral BeF<sub>2</sub> and SiO<sub>2</sub>, and between BeCl<sub>2</sub> and SiS<sub>2</sub>. A whole range of as yet experimentally undiscovered low-energy structures for BeF<sub>2</sub> and BeCl<sub>2</sub>, but also for SiS<sub>2</sub>, were discussed, suggesting that the experimentally observed lack of polymorphism for T<sup>2+</sup>X<sup>2-</sup> materials does not stem from a lack of low-energy polymorphs but more likely is the result of a lack of experimental exploration.

The energetic penalty associated with metastable BeX<sub>2</sub> polymorphs is only half that calculated for the corresponding

SiX<sub>2</sub> ones. We expect therefore that the rich polymorphic chemistry of SiO<sub>2</sub>, in particular for nanoporous frameworks, can be at least matched, if not extended, by BeF<sub>2</sub> provided that synthetic methods are developed that enable the use of organic structure-directing molecules during crystallization of BeF<sub>2</sub>, or other means of kinetic stabilization of open structures.

**Acknowledgment.** We kindly acknowledge Drs. B. Slater, A.A. Sokol, G.A. Tribello and Prof. S.T. Bromley for stimulating discussion. M.A.Z. acknowledges the Spanish Ministry for Science and Innovation (Ministerio de Ciencia e Innovación de Gobierno de España) for a Juan de la Cierva Fellowship.

**Supporting Information Available:** Comparison of the PBE0 calculated and experimentally measured frequencies of the longitudinal phonons in siliceous quartz and PBE0 optimized crystal structures of BeF<sub>2</sub> coesite and low energy porous BeF<sub>2</sub>/BeCl<sub>2</sub>. This material is available free of charge via the Internet at <http://pubs.acs.org>.

JA8026967